

# 水滴撞擊現象對土壤水分入滲之影響

## The Influence of Water Droplet Impact on Soil Water Infiltration

國立屏東技術學院  
資源保育技術系副教授

張 文 詔

Wen-Jaur Chang

### 摘 要

噴灌水滴滴撞擊土壤表面之角度與撞擊面上薄水層對土壤水分入滲率之影響是本報告研究之重點，本報告使用三種不同土壤做水滴不同撞擊角度對土壤水分入滲率影響之測定，測定之水滴撞擊土壤表面角度包括與土壤表面成  $90^\circ$ ， $60^\circ$ ，與 $45^\circ$ 等三種角度，入滲率測定之結果顯示不同水滴撞擊角度會產生不同之土壤水分入滲率，在這三種土壤中其變化情形基本上是  $90^\circ$ 撞擊角度所產生之土壤水分入滲率最大， $45^\circ$ 其次， $60^\circ$ 最小。這些由於不同之水滴撞擊角度所造成不同土壤水分入滲率之現象可以用水滴滴撞擊現象之數值模擬結果來解釋。

### ABSTRACT

The effects of sprinkler droplet impact angle and of a surface water layer in reducing a soil's infiltration rate through soil crustling were studied. Infiltration tests were conducted on three soil types with droplet impact angles of  $90^\circ$ ,  $60^\circ$  and  $45^\circ$ . The results of Infiltration tests revealed that different droplet impact angle caused different soil water infiltration rate. For all soil types, the infiltration rate decreased basically in the following order of impact angle:  $90^\circ$ ,  $45^\circ$  and  $60^\circ$ . The results of these Infiltration tests may be explained by the numerical simulation of water droplet impact mechanism.

### INTRODUCTION

Soil crust formation causes soil water infiltration problems in many arid and semi-arid irrigated areas (Morin et al. 1981). The influence of soil surface crust formation, especially due to the impact of raindrops and irrigation sprinkler droplets, on soil water infiltration has long been a research interest for soil scientists and agricultural engineers. McIntyre (1958a, 1958b) proposed the process of soil crustling and suggested the following important steps during rainfall that reduce

a soil's infiltration rate: (1) wet soil aggregates are broken by droplet impact, (2) surface pores are clogged by wash-in particles, (3) soil surface is compacted by droplet impact, and (4) thin skin crust forms from suspended small soil particles deposited after the rainfall or irrigation has stopped. Based on evidence from electron micrographs of several soil crust samples, Onofiok and Singer (1984) reconstructed the processes leading to soil crust formation which were similar to the

processes proposed by McIntyre (1958a, 1958b) but more specified in sequence.

Soil particle detachment is the first step during the crust formation and also for soil erosion. Soil particle detachment is most often correlated with impact energy (Ekern and Muckenhir 1947; Wischmeier and Smith 1958; Agassi et al. 1985; Thompson and James 1985; Shainberg and Singer 1988; Ben-Hur and Letey 1989). Impact kinetic energy of raindrops may be a good index to predict the amount of soil erosion (Wischmeier 1959, 1976), but from a mechanistic point of view the kinetic energy of a droplet before it impacts on soil surface is not directly related to the physical detachment of soil particles (Ghadiri and Payne 1977). According to Ghadiri and Payne (1977, 1981 and 1986) the interaction of stress generated during droplet impact and shear strength of soil is the major mechanical factor related to physical detachment of soil particles. Al-Durrah and Bradford (1982) reported that lateral shear stress caused by radial flow of the impacting droplet was the major cause of soil particle detachment in droplet impact; splash weight of soil particles is related to both shear stress caused by droplet impact and strength of soil.

Factors that affect crust formation can be divided into two major groups: (1) chemical properties of soil and applied water, and (2) mechanical properties of the soil and the applied water (Agassi et al. 1985; Shainberg and Singer 1988). The first group includes the chemical compositions of soil material and of the water (Aly and Letey 1989). Irrigation waters which contain low levels of dissolved salt or those in which the predominant salt is sodium bicarbonate increase the tendency for crust formation and can also cause reduced permeability below the soil surface due to clay swelling and dispersion (LAWR 1984). The chemical properties of water droplets and soils that influence soil particle detachment are exchangeable sodium percentage (Agassi et al. 1985; Painuli and Abrol 1986; Shainberg and Singer 1988), sodium polymetaphosphate (NaPMP) (Ben-Hur et al. 1986), cationic guar (CP-14) and anionic polyacrylamide (PAM) (Aly and Letey 1989), and salinity of applied water (Helalia et al. 1988, Ben-Hur and Letey 1989). The second

group includes soil physical properties (Cruse and Larson 1977) and mechanical properties of applied water such as water droplet impact mechanics, overland flow shear and energy dissipation in the flow, etc (Ghadiri and Payne 1977; Al-Durrah and Bradford 1982; Ferreira and Singer 1985; Thompson and James 1985). The mechanical properties of water droplet and soil that influence soil particle detachment are commonly correlated with droplet impact energy (Ekern and Muckenhirn 1947; Wischmeier and Smith 1958; Agassi et al. 1985; Thompson and James 1985; Shainberg and Singer 1988; Ben-Hur and Letey 1989). Some recent studies on soil particle detachment queried the traditional impact energy concept (Al-Durrah and Bradford 1982; Huang et al. 1982; Ghadiri and Payne 1977, 1981 and 1986). These authors reported that the shear stress generated during droplet impact and the strength of soil are the major factors related to soil particle detachment. The simulation results of droplet impact do not support the traditional concept that impact kinetic energy is the most important factor in soil particle detachment by water droplet impact (Chang 1990, 1991a,b). Droplets with the same impact velocity (also same impact energy) but different in impact angle ( $90^\circ$ ,  $60^\circ$  and  $45^\circ$ ) or impact surface conditions (bare surface or surface with water layer) generated different impact pressures, impact forces and lateral shear flows. The larger water droplets emitted from sprinkle nozzles usually strike the ground surface at an oblique angle. A better understanding of the effect of sprinkle droplet impact on soil water infiltration may improve sprinkler design or suggest improving an irrigation schedule. This phase of the research focuses on mechanical properties of applied water with an emphasis on sprinkler droplet impact.

In this study a series of infiltration tests were conducted on three different soil types with two stages of impact energy and three different impact angles. The objective of this study was to investigate the influence of sprinkler droplet impact angle on soil water infiltration during irrigation.

## MATERIALS AND METHODS

### *Infiltration Tests*

Three soil types were collected from the San Joaquin Valley in Central California. The schematic of the infiltration test is shown in Fig. 1. Soil samples were air dried, sieved through a 2 mm sieve, and packed loosely in a 51 mm I.D. soil columns (Fig. 2) to simulate the tilled soil surface. There was a 6 mm clearance on the top of packed soil surface, hence a 6 mm depth of water could be ponded during an infiltration test. Soil columns were placed in an outflow collector (Fig. 3). Bulk densities of the packed soil columns were  $1.32 \text{ gm/cm}^3$  for soil type A,  $1.30 \text{ gm/cm}^3$  for soil type B and  $1.51 \text{ gm/cm}^3$  for soil type C. Some physical properties of these 3 soils

are as following:

- Soil A: Sand 40%, Silt 44%, Clay 16%,  
O.M. 1.15%, M.C. 3.6%
- Soil B: Sand 19%, Silt 50%, Clay 31%,  
O.M. 2.05%, M.C. 5.1%
- Soil C: Sand 72%, Silt 17%, Clay 11%,  
O.M. 9.37%, M.C. 1.2%

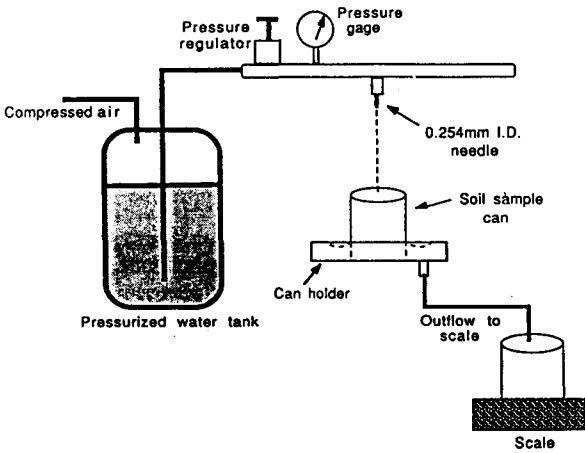


Fig. 1. Infiltration test schematic

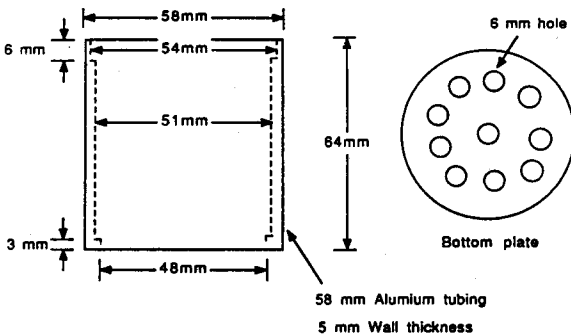


Fig. 2 Schematic of soil column

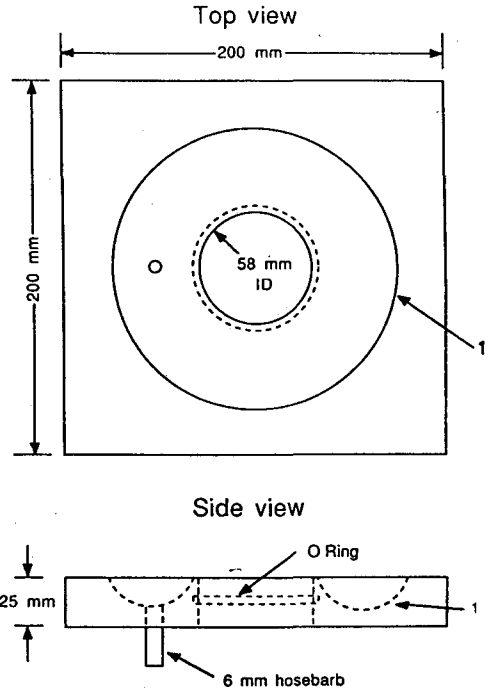


Fig. 3 Schematic of overflow collector

Tap water was applied to the soil column surfaces through a 0.254 mm I.C. needle which was connected to a pressurized water tank (Fig. 1). A pressure regulator was used to maintain stable constant pressure in operation. Two operation pressures were applied, 68.9 KPa (10 psi) and 137.9 KPa (20 psi), which generated two impact velocities: mean droplet impact velocities of 580 cm/sec and 800 cm/sec, respectively. The droplet impact angles and impact velocities were monitored and calculated via a high speed video camera operated at 1000 frames/sec. Infiltration tests were conducted on all soil types for the three impact angles ( $90^\circ$ ,  $60^\circ$  and  $45^\circ$ ) and for no impact condition, in which the soil surface

was covered with a 3 mm thick abrasive scrub cloth and water was applied onto the surface smoothly without any impact. The choice of the three droplet impact angles was based on the report of Chang and Huang (1990) which indicated that the sprinkler droplet impact angles ranged from approximately  $90^\circ$  near the nozzle to approximately  $40^\circ$  near the wetted perimeter. Water application rates were 15.66 ml/min and 32.91 ml/min for low and high impact velocities, respectively. Infiltration rates were calculated by subtracting overflow rates from inflow rates. Overflow weight was measured with a Mettler PM 2000 electrical scale recorded every minute. The duration of each infiltration test was 30 minutes. Five replications were conducted on each soil type with the three impact angles at low impact velocity levels. Three replications were conducted on each soil type with the three impact angles at high impact velocity levels. In total 87 tests were conducted.

## RESULTS AND DISCUSSION

### *Infiltration Test*

The infiltration rates of the three soils, at two levels of impact velocities and three impact angles of water application together with the no impact condition were calculated (Figs. 4, 5 and 6). Also, a statistical table (Table 1) of final infiltration rates, 20 minutes after the beginning of the tests, was made to show the relationship between infiltration rates and droplet impact angles. Means and standard deviations of final infiltration rates were calculated. Several experimental observations about the influence of droplet impact on infiltration were made:

(1) There are four observed stages during infiltration tests: (i) Before water ponding, water droplets impacted onto the bare soil surface, soil particles were disaggregated, and impact water was sucked into the soil layer rapidly. (ii) As droplet impact continued soil surface conductivity decreased, ponding started, and soil particle detachment continued. (iii) Ponding depth exceeded 6 mm depth and overflow began, some disaggregated soil particles followed the infiltrated water "washed in" to the top soil layer to clog soil pores. Some disaggregated soil particles deposited on the soil surface to form a thin skin

crust. Some deposited skin crust was disturbed and resuspended depending on droplet impact conditions. (iv) Approximately 20 minutes after the test began the infiltration rate reached a relatively steady state.

(2) During the infiltration tests of high impact velocity level, the overflow stage occurred sooner than for the low impact velocity stage; for example soil type A needed 1 minutes at the high impact velocity level to reach overflow stage while 3 minutes were needed for low impact velocity level and 5 minutes were needed for the no impact condition to reach overflow stage.

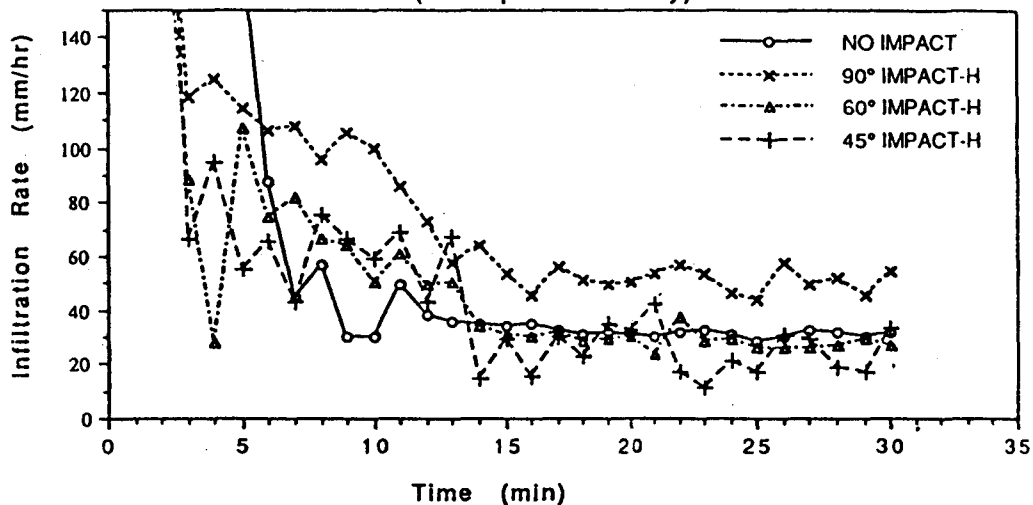
(3) Infiltration rate fluctuation for the three different impact angles was greater than that for the no impact condition. The test with impact angle of  $45^\circ$  had the largest standard deviation. The mean final infiltration rate (20 minutes after the beginning of tests) of all soil types at the low impact velocity level increased in the following order:  $60^\circ$ ,  $45^\circ$ ,  $90^\circ$ , and no impact.

(4) When high impact velocity level was applied, the tendency of infiltration rate of soil type C was similar to that of all soil types at low impact velocity level. The final infiltration rate of high impact velocity is close to that at low impact velocity for soil type C with each impact angle.

(5) When high impact velocity level was applied on soil types A and B, the final infiltration rate of  $90^\circ$  impact was greater than that of no impact and decreased as impact angle decreased. The final infiltration rate at high impact velocity was greater than that at low impact velocity for soil types A and B with each impact angle.

These experimental observations are explained as follows: At the beginning of the test when the droplet was impacting onto the bare soil surface the hydraulic conductivity was high, due to the high water content-matric potential gradient (Borchert et al. 1984). Hence, the applied water was sucked into soil column and no ponding happened during this stage. The droplet impact had two effects on infiltration in this stage: (i) the droplet impact force (integration of impact pressure over impact surface) compacted the top layer of soil surface which impeded water intake; the effective area was limited only to impact contact area (Chang 1991b). (ii) Shear

Infiltration Rate of Soil - A  
(Hi-impact velocity)



Infiltration Rate of Soil - A  
(Lo-impact velocity)

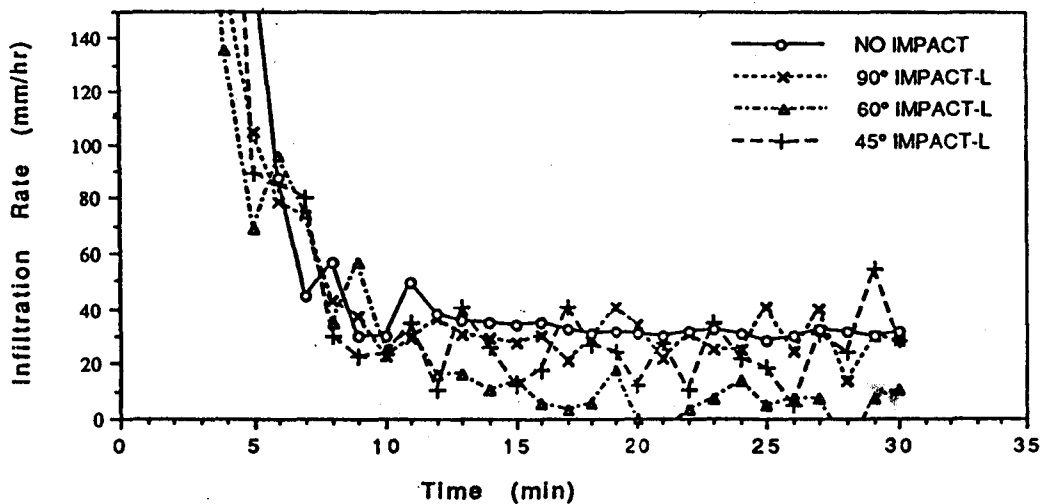
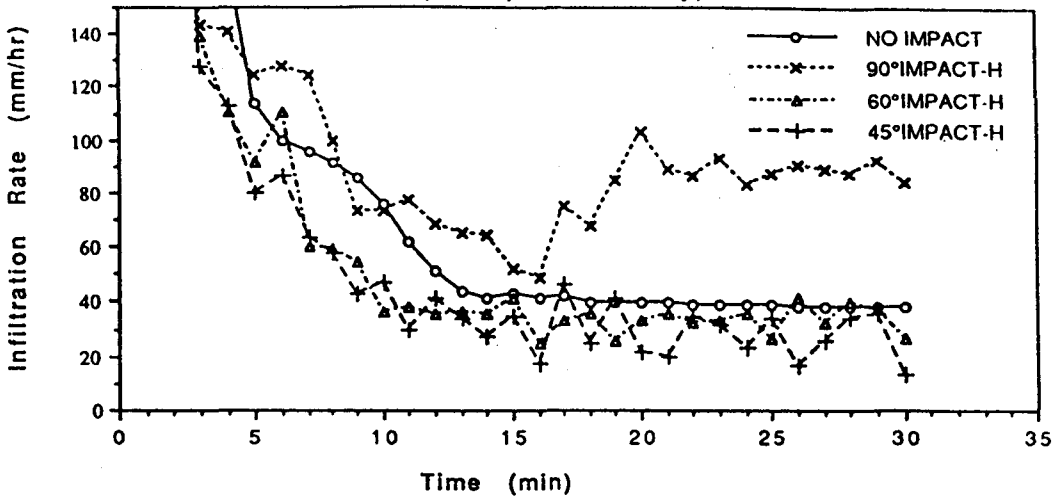


Fig. 4 Infiltration rates of soil A with different impact angles.  
(a) High impact velocity. (b) Low impact velocity.

**Infiltration Rate of Soil - B  
(Hi-impact velocity)**



**Infiltration Rate of Soil - B  
(Lo-impact velocity)**

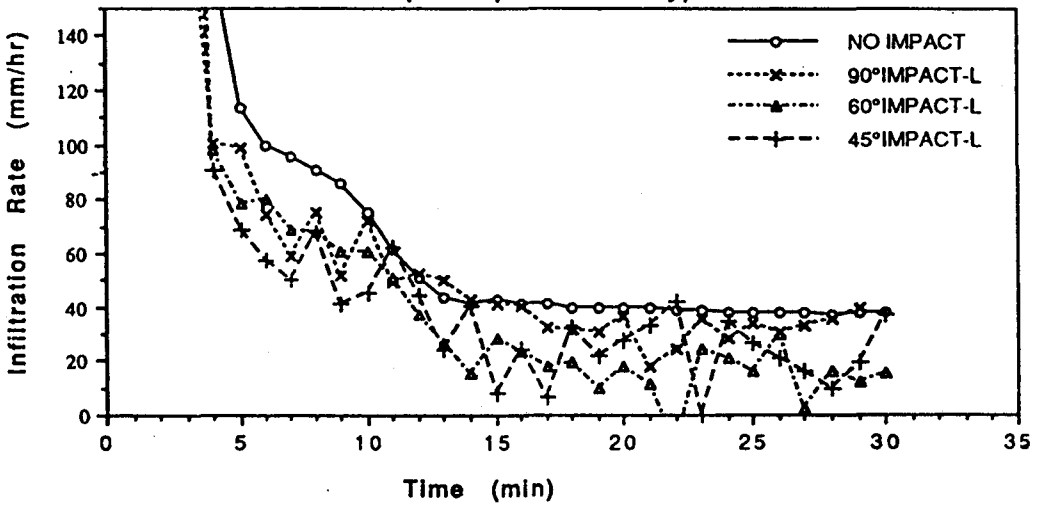
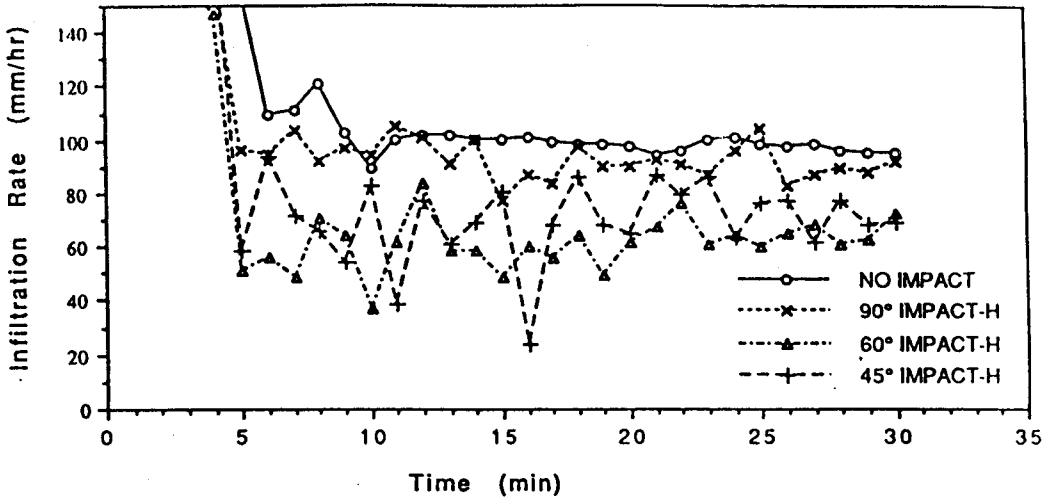


Fig. 5 Infiltration rates of soil B with different impact angles.  
(a) High impact velocity. (b) Low impact velocity

Infiltration Rate of Soil - C  
(Hi-impact velocity)



Infiltration Rate of Soil - C  
(Lo-impact velocity)

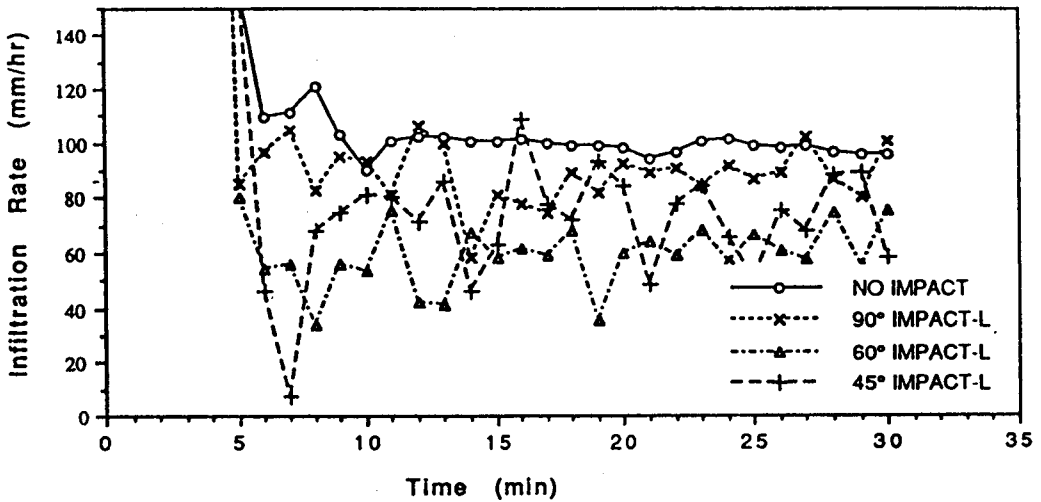


Fig. 6 Infiltration rate of soil C with different impact angles.  
(a) High impact velocity. (b) Low impact velocity.

Table 1. Final infiltration rate of the three soil types (mm/hr)

		Low Impact Velocity		High Impact Velocity	
		MEAN	STD.	MEAN	STD.
SOIL-A	No-Impact	32.97	1.25	32.97	1.25
	90°-Impact	29.56	6.96	51.20	4.87
	60°-Impact	10.14	3.93	27.98	3.60
	45°-Impact	27.26	6.54	23.72	9.62
SOIL-B	No-Impact	38.51	0.68	38.51	0.68
	90°-Impact	31.53	3.88	88.39	3.22
	60°-Impact	13.63	6.47	33.92	4.72
	45°-Impact	20.56	8.01	26.64	8.20
SOIL-C	No-Impact	102.10	2.30	102.10	2.30
	90°-Impact	102.98	3.71	91.39	5.83
	60°-Impact	61.61	4.35	65.92	5.37
	45°-Impact	77.55	11.47	74.83	8.88

stress generated during droplet impact disaggregated soil particles. As infiltration tests continued some of these soil particles washed into the top soil layer and clogged soil pores to form a "wash in zone," and some of these soil particles deposited on the surface to form a thin skin crust (McIntyre 1958b; Onofiok and Singer 1984). The shear stress exceeded soil strength to disaggregate soil particles (Al-Durrah and Bradford 1982). According to Ghadiri and Payne (1986) raindrop impact shear stress is always greater than soil strength hence soil particle detachment is unavoidable when droplets impact on bare soil surface. For the sprinkler droplet impact numerical simulations (Chang 1991b) the 60° impact angle generated the greatest maximum shear velocity (1.69 times greater than the impact velocity) among three impact angles simulated when droplets impacted on the bare surface. This may imply that a 60° impact on bare surface has the greatest potential to disaggregate soil particles.

When infiltration rate decreased, due to the change of water content-matric potential gradient and the influence of droplet impact to less than water application rate, ponding began. The high velocity impact has a higher potential to detach soil particles, and hence, high velocity impact has a shorter time to reach ponding and an over-

flow stage which agrees with Thompson and James (1985). The fluctuation of measured infiltration rate is possibly due to the water surface tension that restricted water flow from the top of soil column to the overflow collector and from the overflow collector to scale.

The ponded water buffered the droplet impact pressure but the total impact force was increased (Chang 1991b). Droplet impact on the ponding surface had two contradictory effects on soil water infiltration. First, impact force caused compaction of the soil surface which impeded water intake, the same effect as on bare surface but effective area is larger. Second, droplet impact increased pressure distribution on the soil surface which, according to Darcy's law, increases infiltration rate. The influence of impact pressure on infiltration is not clearly addressed in the literature. The larger impact pressure distribution on soil surface of 90° impact is a possible reason to cause higher final infiltration rates than for other impact angles.

The infiltration tests with a 60° impact angle had the lowest final infiltration rate in low impact velocity situation and can be explained by: (i) the 60° impact may have disaggregated more soil particles than other impact angles when impacted on bare surface, (ii) after ponding over the soil surface some of disaggregated soil parti-



cles may deposit back on the surface to impede water intake.

The final infiltration rate of high impact velocity tests was higher than for the low impact velocity tests in soil types A and B except for the 45° impact of soil type A. This experimental observation seems to conflict with other researchers' results (Mohammed and Kohl 1986; Shainberg and Singer 1988; Ben-Hur and Letey 1989). Most studies on the influence of water droplet impact on soil water infiltration stated that higher impact kinetic energy of droplets (higher droplet impact velocity) decrease infiltration rate, but physical explanations for this conclusion are not clearly addressed in the literature. One possible explanation is that higher impact velocities will indeed disaggregate more soil particles due to higher shear stress generated during impact, but after ponding the disaggregated soil particles have a chance to deposit back on soil surface (this happened in the infiltration test at a lower impact velocity level). Although the water layer over the soil surface buffered shear stress, the high impact velocity still generated a large enough shear stress on the soil surface to prevent deposition of skin crust (this happened in the infiltration test at a high impact velocity level). A skin crust on the soil surface is a more significant factor affecting infiltration rate than clogging of pores by clay migration (Helalia et al. 1988). If the deposit of skin crust is prevented by high impact shear stress, due to high impact velocity, infiltration rate increases as impact pressure increases. The impact pattern is another important factor affecting crust deposition. If only limited spots are subjected to droplet impact in the infiltration area, then higher impact velocity (higher impact kinetic energy) disaggregated more soil particles before ponding which are then deposited after ponding in spots where no impact occurs; therefore, more skin crust was formed than that formed with a low impact velocity, and water intake impedance increases with increasing impact energy. This can be used to explain the studies of Shainberg and Singer (1988) and Ben-Hur and Letey (1989); both reported that infiltration rate decreased with increasing impact energy. But when droplet impact density was

increased (increasing the area subject to droplet impact), higher impact velocity (greater impact kinetic energy, shear stress, and pressure distribution) may decrease the degree of crust deposition after ponding. In this situation, higher pressure distribution due to higher impact energy may actually increase the final infiltration rate. Mohammed and Kohl (1986) used different nozzles to generate different impact energy levels in field infiltration tests; they stated that infiltration rate decreased with increasing impact energy, but when they increased the number of nozzles (increase the number of droplet impact spots) to increase the water application intensity at the same impact energy level, then the infiltration rate increased with increasing water application intensity. Romkens et al. (1985) used a multiple-intensity rain fall simulator (Meyer and Harmon 1979) in laboratory infiltration tests and showed that higher intensity caused higher infiltration rates. These results support our explanations above.

Droplet impact shear stress must exceed soil strength to detach soil particles or to remove the deposited skin crust (Al-Durrah and Bradford 1982). The effective area of shear stress was calculated (Figs. 7 and 8) from the droplet impact numerical simulation results (Chang 1991b). The effective area of shear stress greater than 1.0 dyne/cm<sup>2</sup> is almost equal to zero for low velocity impact on 6 mm water layer (Fig. 7). If the shear strength of the skin crust was near this value then the degree of skin crust removal would be small. For a high impact velocity level with a 45° impact the effective area of shear stress greater than 1.0 dyne/cm<sup>2</sup> is equal to zero. If the crust shear strength of soil type A was greater than or equal to 1.0 dyne/cm<sup>2</sup> then the degree of crust removal for a 45° impact would be small. The final infiltration rate of soil type A in 45° impact at higher impact velocity level was less than that at low impact velocity level. For soil type C sand is the major component (72%) in the soil texture which consolidates rapidly (Hillel 1982) and a rougher skin crust is deposited. This feature of soil surface microrelief may have some influence on the deposited skin crust removal (Huang et al. 1982). One possible explanation is that the rough sur-

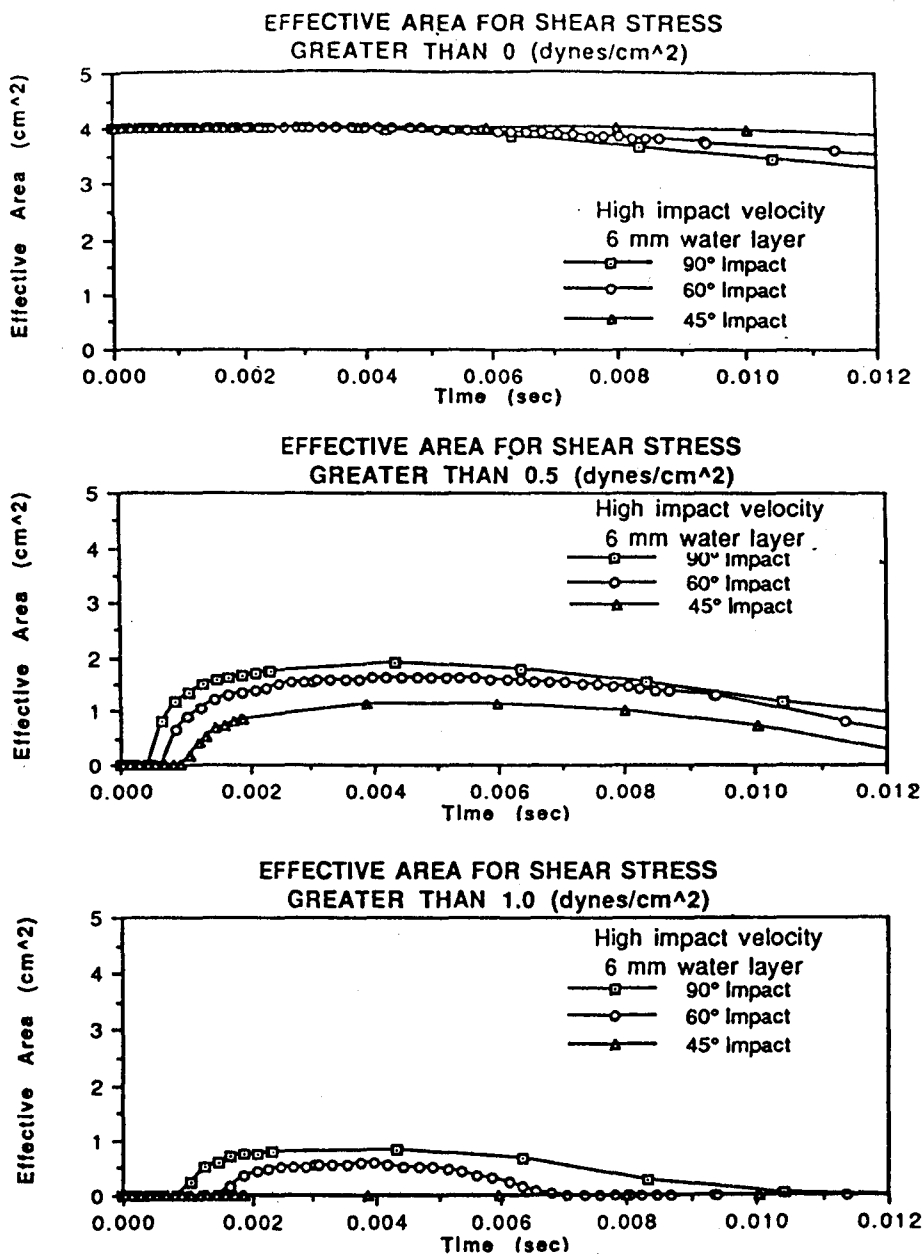


Fig. 7 Shear stress effective area of 4 mm droplet impact with  $V=800\text{cm/sec}$  and depth of water layer = 6 mm.

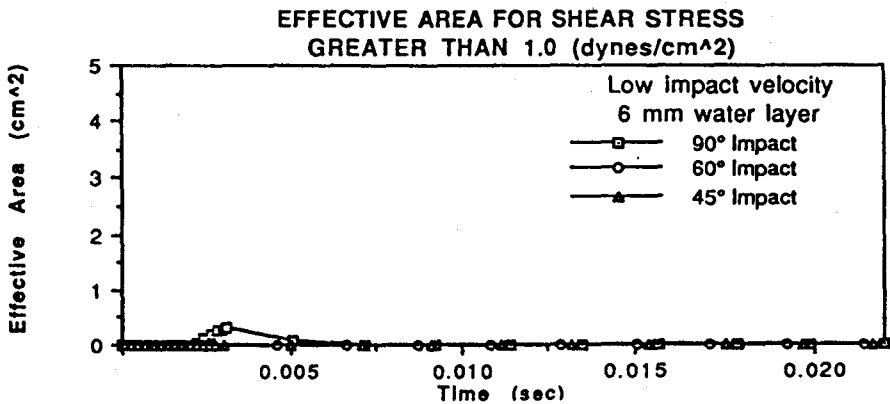
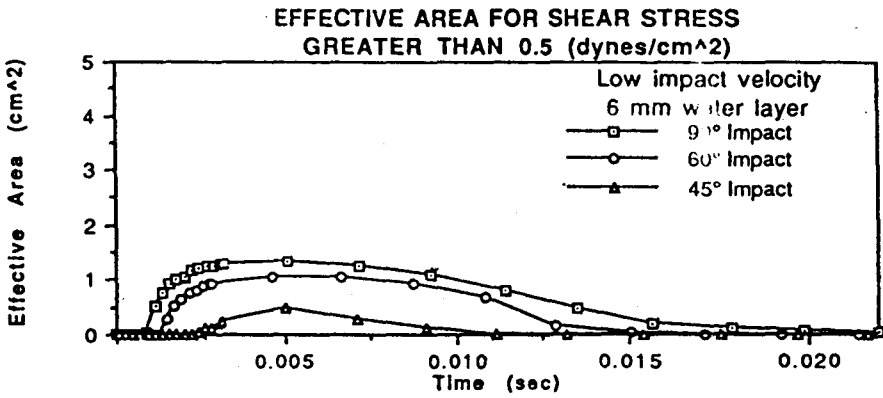
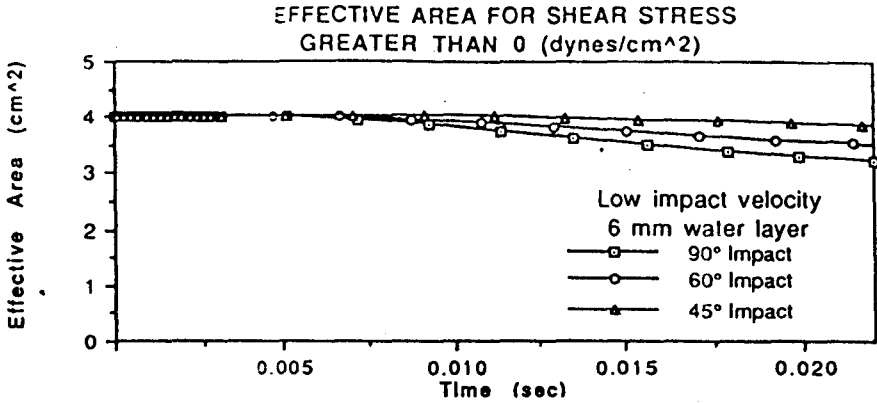


Fig. 8 Shear stress effective area of 4 mm droplet impact with  $V=580\text{cm/sec}$  and depth of water layer = 6 mm.

face obstructs the transmission of shear stress which prevents most skin crust from being resuspended even at high impact velocity level. Thus, the influence of droplet impact angle on infiltration rate in soil C is similar to that in soil A and B at low impact velocity level.

## CONCLUSION

### Conclusions:

1. The mean final infiltration rate (20 minutes after the beginning of tests) of all soil types at the low impact velocity level increases in the following order: 60°, 45°, 90° and no impact.
2. When high impact velocity level is applied, the tendency of infiltration rate of soil type C is similar to that of all soil types at low impact velocity level. The final infiltration rate at high impact velocity is close to that at low impact velocity for soil type C with each impact angle.
3. When a high impact velocity level is applied to soil types A and B, the final infiltration rates of 90° impact are greater than of no impact and decreases as impact angle decreases. The final infiltration rates at high impact velocity are greater than that at low impact velocity for soil types A and B with each impact angle.
4. If skin crust does not deposit after ponding then a higher impact velocity (higher impact energy) will cause higher infiltration due to higher impact pressure distribution over the soil surface.

### REFERENCE

1. Agassi, M., I. Shainberg, and J. Morin, 1981. Effect of electrolyte concentration and soil sodicity on the infiltration rate and crust formation. *Soil Sci. Am. Soc. J.* 45: 1848-851.
1. Agassi, M., J. Morin, and I. Shainberg. 1985. Effect of raindrop impact energy and water salinity on infiltration rates of sodic soils. *Soil Sci. Am. Soc. J.* 49: 186-190.
3. Al-Durrah, M. M. and J. M. Bradford. 1982. The mechanism of raindrop splash on soil surface. *Soil Sci. Soc. Am. J.* 46: 1086-

- 1099.
4. Aly, S. M. and J. Letey. 1989. The effect of two polymers and water qualities on dry cohesive strength of three soils. *Soil Sci. Soc. Am. J.* 53: 255-259.
5. Ben-Hur, M., I. Shainberg, and R. Kern. 1986. Effect of sodium polymetaphosphate on soil crust formation and runoff/rain relations. *Soil Sci. Soc. Am. J.* 50: 1314-1318.
6. Ben-Hur, M. and J. Letey. 1989. Effect of polysaccharides, clay dispersion, and impact energy on water infiltration. *Soil Sci. Am. Soc. J.* 53: 233-238.
7. Borchert, C. A., J. Skopp, D. Watts and J. Schepers. 1984. Determining unsaturated hydraulic conductivity for fine textured soils. ASAE Paper No. 84-2513. St. Joseph, MI.
8. Chang, W. J. 1990. Numerical simulation water droplet impact on rigid surface I: Simulation method. *J. Chinese Soil and Water Conservation.* 21(2): 1-27.
9. Chang, W. J. and C. T. Huang. 1990. Study on impact angles of sprinkler droplet. *J. Chinese Soil and Water Conservation.* 21(2): 46-56.
10. Chang, W. J. 1991a. Analysis of droplet impact and its effect on water infiltration during sprinkler irrigation. Ph. D. Dissertation University of California. Davis.
11. Chang, W. J. 1991b. Numerical simulation of water droplet impact on rigid surface II: The influence of droplet impact angle and water film thickness on droplet impact mechanism. *J. Chinese Soil and Water Conservation.* in press.
12. Cruse, R. M. and W. E. Larson. 1977. Effect of soil shear strength on soil detachment due to raindrop impact. *Soil Sci. Soc. Am. J.* 41: 777-781.
13. Ekern, Jr. P. C. and R. J. Muckenhirn. 1947. Water drop impact as a force in transporting sand. *Soil Sci. Soc. Am. Proc.* 12: 441-444.
14. Ferreira, A. G. and M. J. Singer. 1985. Energy dissipation for water drop impact into shallow pools. *Soil Sci. Soc. Am. J.* 49: 1537-1542.
15. Ghadiri, H. and D. Payne. 1977. Raindrop impact stress and the breakdown of soil

- crumbs. *J. Soil Science*. 28: 247-258.
16. Ghadiri, H. and D. Payne. 1981. Raindrop impact stress. *J. Soil Science* 32: 41-49.
  17. Ghadiri, H. and D. Payne. 1986. The risk of leaving the soil surface unprotected against falling rain. *Soil and Tillage Research*. 8: 119-130.
  18. Helalia, A. M., J. Letey, and R. C. Graham. 1988. Crust formation and clay migration effects on infiltration rate. *Soil Sci. Am. Soc. J.* 52: 251-255.
  19. Hillel, D. 1982. Introduction to soil physics. Academic Press. Orlando.
  20. Huang, C., J. M. Bradford. and J. H. Cushman. 1982. A numerical study of raindrop impact phenomena: The rigid case. *Soil Sci. Soc. Am. J.* 46: 14-19.
  21. Dept. of Land, Air and Water Resource. 1984. Water penetration problems in California soils. Univ. of California Davis. Technical Report 10011.
  22. McIntyre 1958a. Permeability measurements of soil crusts formed by raindrop impact. *Soil Science*, 85(4): 185-189.
  23. McIntyre, D. S. 1958b. Soil splash and the formation of surface crusts by raindrop impact. *Soil Sci.* 85: 261-266.
  24. Meyer, L. D. and W. C. Harmon. 1979. Multiple-intensity rainfall simulator for erosion research on row sideslopes. *Trans. A. S. A. E.* 22(1): 100-103.
  25. Mohammed, D. and R. A. Kohl. 1986. Infiltration response to kinetic energy. ASAE Paper No. 86-2106. St. Joseph, MI.
  26. Morin, J., Y. Benyamini, and A. Michaeli. 1981. The effect of raindrop impact on the dynamics of soil surface crusting and water movement in the profile. *J. Hydrol.* 52: 324-335.
  27. Onofolk, O., and M. J. Singer. 1984. Scanning electron microscope studies of soil surface crusts formed by simulated rainfall. *Soil Sci. Soc. Am. J.* 48: 1137-1143.
  28. Painuli, D. K. and I. P. Abrol. 1986. Effects of exchangeable sodium on crusting behaviour of a sady loam soil. *Aust. J. Soil Res.* 24: 367-376.
  29. Romkens, M. J. M., R. L. Baumhardt, M. B. Parlange, F. D. Whisler, J. Y. Parlange and S. N. Prasad. 1986. Rain-induced surface seals: their effect on ponding and infiltration. *Annales Geophysicae*. 4, B, 4, 417-424.
  30. Shainberg, I. and M. J. Singer. 1988. Drop impact energy-soil exchangeable sodium percentage interactions in seal formation. *Soil Sci. Soc. Am. J.* 52: 1449-1452.
  31. Thompson, A. L. and L. G. James. 1985. Water droplet impact and its effect on infiltration. *Trans. A. S. A. E.* 28(5): 1506-1510, 1520.
  32. Wischmeier, W. H. and D. D. Smith. 1958. Rainfall energy and its relationship to soil loss. *Trans. Am. Geo. Union.* 39(2): 285-291.
  33. Wischmeier, W. H. 1959. A rainfall erosion index for a universal soil loss equation. *Proc. Soil Sci. Soc. Am.* 23: 246-249.
  34. Wischmeier, W. H. 1976. Use and misuse of the universal soil loss equation. *J. Soil and Water Conserv.* 31: 5-9.

收稿日期：民國80年11月8日

修改日期：民國80年11月22日

接受日期：民國80年12月11日

專營土木、水利、建築等工程

東霸營造有限公司

負責人：李文龍

地址：花蓮市富裕五街109號

電話：(038)560676

專營土木、水利、建築等工程

宏偉土木包工業

負責人：莊訓倫

地址：花蓮縣吉安鄉北昌村

北昌三街58號

電話：(038)353636